Taylor & Francis
Taylor & Francis Group

RESEARCH PAPER

 OPEN ACCESS

TRPA1 is functionally co-expressed with TRPV1 in cardiac muscle: Co-localization at z-discs, costameres and intercalated discs

Spencer R. Andrei[a], Pritam Sinharoy[a], Ian N. Bratz[b], and Derek S. Damron[a]

[a]Department of Biological Sciences, Kent State University, Kent, OH, USA; [b]Department of Integrated Medical Sciences, Northeast Ohio Medical University, Rootstown, OH, USA

ABSTRACT

Transient receptor potential channels of the ankyrin subtype-1 (TRPA1) and vanilloid subtype-1 (TRPV1) are structurally related, non-selective cation channels that show a high permeability to calcium. Previous studies indicate that TRP channels play a prominent role in the regulation of cardiovascular dynamics and homeostasis, but also contribute to the pathophysiology of many diseases and disorders within the cardiovascular system. However, no studies to date have identified the functional expression and/or intracellular localization of TRPA1 in primary adult mouse ventricular cardiomyocytes (CMs). Although TRPV1 has been implicated in the regulation of cardiac function, there is a paucity of information regarding functional expression and localization of TRPV1 in adult CMs. Our current studies demonstrate that TRPA1 and TRPV1 ion channels are co-expressed at the protein level in CMs and both channels are expressed throughout the endocardium, myocardium and epicardium. Moreover, immunocytochemical localization demonstrates that both channels predominantly colocalize at the Z-discs, costameres and intercalated discs. Furthermore, specific TRPA1 and TRPV1 agonists elicit dose-dependent, transient rises in intracellular free calcium concentration ($[Ca^{2+}]_i$) that are abolished in CMs obtained from TRPA1$^{-/-}$ and TRPV1$^{-/-}$ mice. Similarly, we observed a dose-dependent attenuation of the TRPA1 and TRPV1 agonist-induced increase in $[Ca^{2+}]_i$ when WT CMs were pretreated with increasing concentrations of selective TRPA1 or TRPV1 channel antagonists. In summary, these findings demonstrate functional expression and the precise ultrastructural localization of TRPA1 and TRPV1 ion channels in freshly isolated mouse CMs. Crosstalk between TRPA1 and TRPV1 may be important in mediating cellular signaling events in cardiac muscle.

Introduction

Transient receptor potential (TRP) ion channels of the ankyrin 1 (TRPA1) and vanilloid 1 (TRPV1) subtypes are members of the TRP superfamily of structurally related, non-selective cation channels first described in sensory neurons that are highly permeable to calcium.[1] Recent evidence suggests that TRPA1 and TRPV1 receptors exhibit reciprocal regulation, indicating cross-talk between the 2 receptors when co-expressed in the same cell[2,3] and both channels play an important role in the induction of neurogenic pain and inflammation.[4-10] However, there is accumulating evidence that TRPA1 and TRPV1 have functional roles independent of sensory neurons. In fact, emerging evidence indicates TRPA1 and TRPV1 are expressed in various of other cell types including smooth muscle cells and endothelial cells.[11]

To our knowledge the expression of TRPA1 at the protein level in cardiac muscle as well as evidence identifying the functionality of the channel and its ultrastructural location in CMs has yet to be described. One recent study identified the presence of TRPA1 mRNA in mouse CMs,[12] whereas only one other study has demonstrated expression of TRPA1 at the protein level in cardiac fibroblasts.[13] However, several studies conducted over the past decade have demonstrated a cardioprotective role for TRPV1 in the setting of myocardial ischemia and reperfusion injury[14] in addition to attenuating high salt-induced cardiac hypertrophy[15,16] and ameliorating pressure overload-induced

hypertrophy.[17,18] Moreover, TRPV1 channels have recently been described to primarily localize near the epicardial surface of the heart,[19] however the precise location of the TRPV1 channels within the ultrastructure of the cardiomyocyte (CM) has yet to be reported. Since evidence exists in sensory neurons and heterologous expression systems that TRPA1 and TRPV1 may cross-regulate each other's function serving as "partners in crime",[20,21] we questioned whether the potential for a similar paradigm may exist if in fact TRPA1 is coexpressed with TRPV1 in adult mouse CM's. Uncovering the precise location of TRPA1 and TRPV1 within the ultrastructure of the CM could provide important information as to the specific role(s) the channels mediate in physiological and/or pathophysiological events in the heart.

In the current study, we examined the extent to which TRPA1 and TRPV1 are co-expressed in adult mouse CM's, assessed whether they are expressed throughout the entire myocardium or localized to specific layers of the heart and identified their precise ultrastructural location within the isolated CM cytoskeleton. Moreover, we have explored the extent to which TRPA1 and TRPV1 are functionally active by assessing changes in intracellular free Ca^{2+} concentration ($[Ca^{2+}]_i$ in response to increasing concentrations of allyl isothiocyanate (AITC; specific TRPA1 agonist) or capsaicin (specific TRPV1 agonist) in CM's obtained from WT as well as TRPA1$^{-/-}$ and TRPV1$^{-/-}$ mice. Dose response curves for TRPA1 channel inhibition (HC-030031) or TRPV1 channel inhibition (SB366791) on the agonist-induced rises in $[Ca^{2+}]_I$ were also performed in CM's obtained from WT mice. The major findings of the current study are that both TRPA1 and TRPV1 are co-expressed in CMs throughout the endocardium, myocardium and epicardium and appear to specifically colocalize at the Z-discs and costameres. Moreover, both TRPA1 and TRPV1 agonists elicit transient rises in $[Ca^{2+}]_i$ that are absent in CMs obtained from TRPA1$^{-/-}$ and TRPV1$^{-/-}$ mice and attenuated in a dose-dependent manner in WT CMs pretreated with specific TRPA1 and TRPV1 channel antagonists. The current studies will lay the foundation for future studies investigating the extent to which cross-talk/regulation between TRPA1 and TRPV1 play a role in mediating the physiology and pathophysiology of cardiac tissue.

Results

TRPA1 and TRPV1 are expressed in CMs

Representative immunoblots demonstrating the expression of TRPA1 and TRPV1 in CMs are shown in Figures 1A–B. CMs obtained from WT, TRPA1$^{-/-}$ and TRPV1$^{-/-}$ mice were lysed and prepared for immunoblotting using antibodies recognizing TRPA1 or TRPV1. Non-transfected F-11 cells and F-11 cells
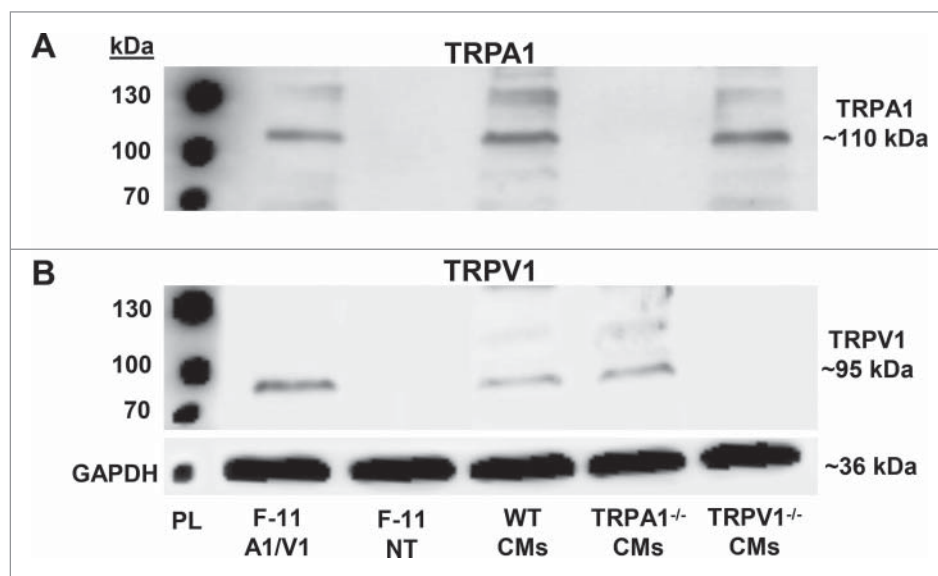
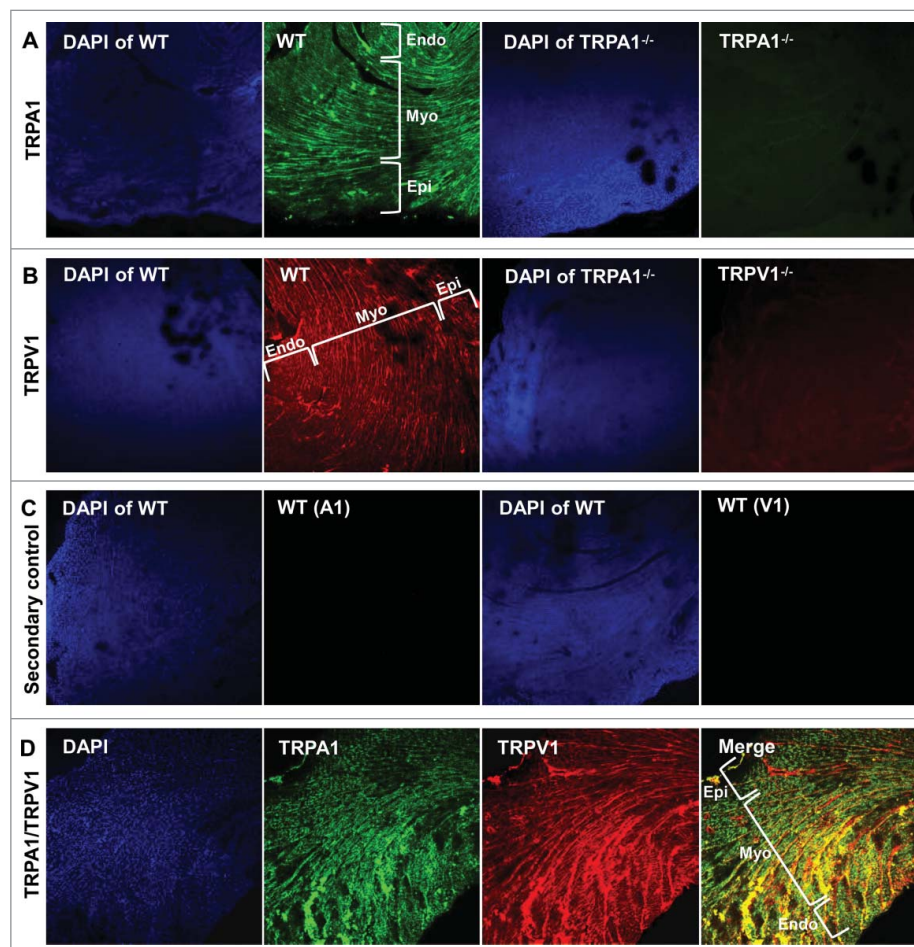**Figure 1.** Representative immunoblots depicting TRPA1 and TRPV1 expression in adult mouse ventricular cardiomyocytes (CMs). Representative immunoblots demonstrating TRPA1 (A) and TRPV1 (B) expression in F-11 cells transfected with TRPA1 and TRPV1 (F-11 A1/V1), non-transfected F-11 cells (F-11 NT), wild-type (WT) CMs, TRPA1$^{-/-}$ CMs and TRPV1$^{-/-}$ CMs. GAPDH was probed as the loading control. PL = protein ladder.

transfected with TRPA1 and TRPV1 served as the negative and positive controls, respectively. Immunoblot analysis demonstrated expression of TRPA1 at 110 kDa (Fig. 1A) and subsequent reprobing of TRPV1 at 95 kDa (Fig. 1B).

TRPA1 and TRPV1 colocalize in cardiac tissue

Mid-ventricular heart sections obtained from WT, TRPA1$^{-/-}$ and TRPV1$^{-/-}$ mice were subjected to anti-TRPA1 and/or anti-TRPV1 antibodies and prepared for immunohistochemical analysis (Fig. 2). DAPI was used to label nuclei. Immunohistochemical staining of TRPA1 or TRPV1 in sections obtained from WT, TRPA1$^{-/-}$ and TRPV1$^{-/-}$ mice are shown in Figure 2A–B and illustrate the presence of TRPA1 and TRPV1 throughout the heart in sections obtained from WT mice whereas no

immunodetectable staining was evident for TRPA1 or TRPV1 in the sections obtained from TRPA1$^{-/-}$ or TRPV1$^{-/-}$ mice respectively. WT heart sections were also exposed to secondary antibodies in the absence of TRPA1 and TRPV1 primary antibodies, which yielded no immunodetectable labeling (Fig. 2C). Mid-ventricular heart sections obtained from WT mice that were incubated with both anti-TRPA1 and anti-TRPV1 antibodies are also illustrated in Figure 2D indicating colocalization of TRPA1 and TRPV1 throughout the endocardium, mid-myocardium and epicardium. Upon further examination through acquisition of serial confocal Z-stack images of the sections to assess physical depth of tissue staining we observed that both TRPA1 and TRPV1 appear to be localized at the costameres and the Z-discs (Fig. 3A–B). Finally, immunocytochemical assessment of the precise cytoskeletal localization of TRPA1 and

Figure 2. Representative confocal images (10X magnification) obtained from WT mouse hearts depicting immunolocalization of TRPA and TRPV1 in the endocardium (Endo), myocardium (Myo) and epicardium (Epi). Thirty μm sections were labeled with antibody recognizing TRPA1 (green; A) or TRPV1 (red; B) in hearts obtained from WT, TRPA1$^{-/-}$ and TRPV1$^{-/-}$ mice. WT heart sections were also treated with secondary antibody in the absence of primary (C). DAPI was used for nuclear staining. Representative confocal images of double-stained sections indicate that immunodetectable TRPA1 and TRPV1 colocalize throughout cardiac tissue (D).
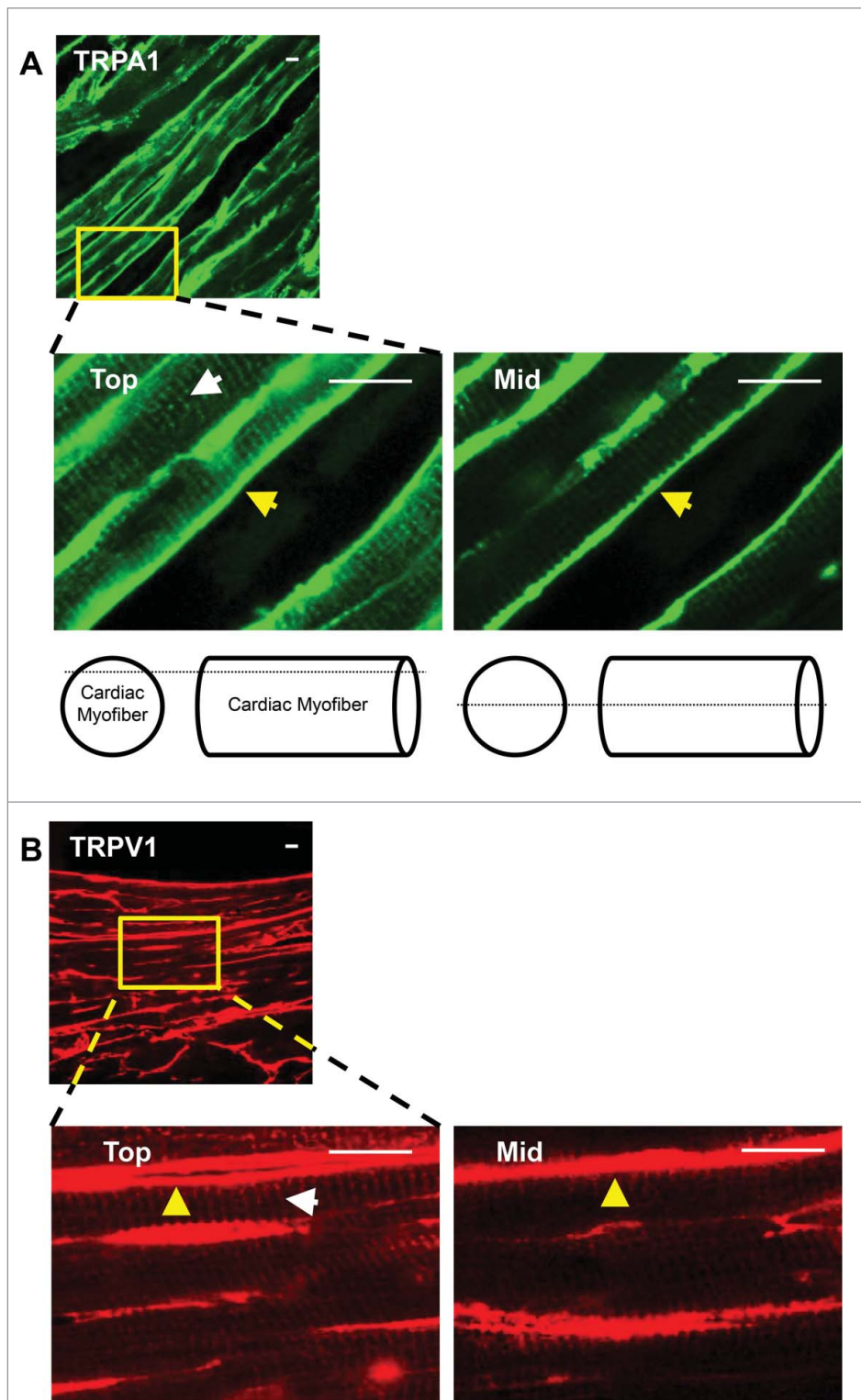
Figure 3. Representative confocal Z-stack images obtained from WT hearts to assess the physical depth of tissue staining reveals that TRPA1 and TRPV1 localize at the costameres (yellow arrows) and Z-discs (white arrows) within the tube-like structure of cardiac myofibers. Heart sections (30 μm) were labeled with antibody recognizing TRPA1 (green; A) or TRPV1 (red; B) and images were acquired at the top and middle (Mid) layers of the myofiber. The lack of Z-disc staining at the middle-levels indicate TRPA1 and TRPV1 predominantly localize toward the outer Z-discs and associated costameric complexes in cardiac tissue. Scale bar, 10 μm.

TRPV1 was performed in freshly isolated CMs. In these studies, CMs were immunostained with anti-α-actinin (Z-disc marker), anti-vinculin (costamere and intercalated disc marker), anti-TRPA1 and/or anti-
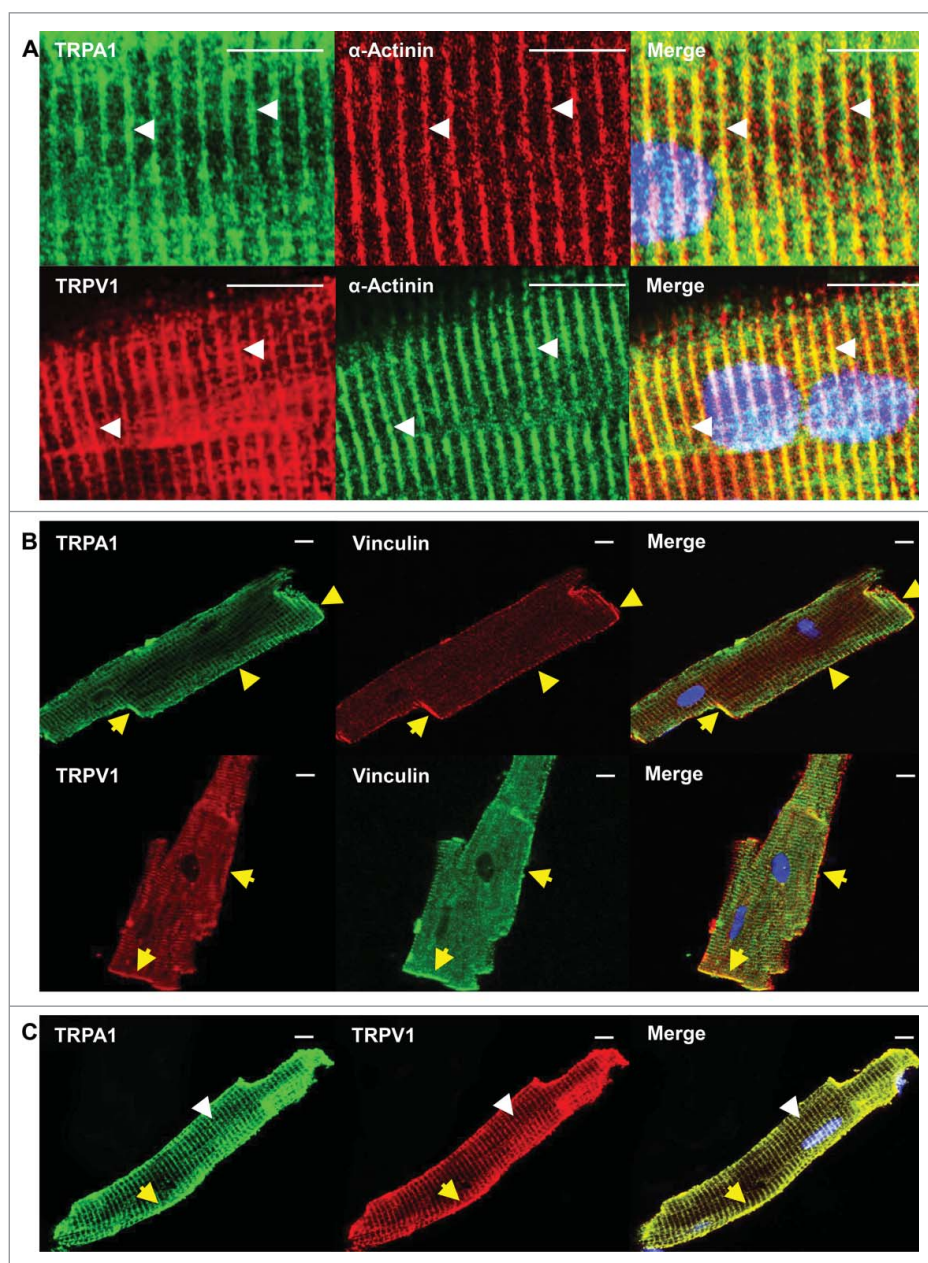
Figure 4. Confocal images in CM obtained from WT mice confirm that TRPA1 and TRPV1 colocalize at the Z-disc, costameres as well as the intercalated discs. Freshly isolated CMs were double labeled with antibody recognizing TRPA1 or TRPV1 and α-actinin (z-disc marker; white arrows) A). Similar immunolabeling with antibody recognizing TRPA1 or TRPV1 and vinculin (costamere and intercalated disc marker, yellow arrow) was also performed (B). Representative confocal images of double-labeled CMs revealed that TRPA1 and TRPV1 colocalize at the Z-disc, costamere, and intercalated discs (C). Scale bar, 10 μm.

TRPV1 (Fig. 4). Figures 4A–B demonstrates colocalization of both TRPA1 and TRPV1 with α-actinin (panel A) indicating localization of both channels at the z-disc in addition to both channels also colocalizing with vinculin (panel B) indicating their presence at the costameres and intercalated disc. Confirmation of the coexpression of TRPA1 and TRPV1 channels in CMs and their co-localization at the z-discs, costameres and intercalated discs is demonstrated in Figure 4C.

### TRPA1 and TRPV1 agonists elicit dose-dependent transient rises in [Ca²⁺]ᵢ in CMs

To examine the extent to which TRPA1 and TRPV1 channels are physiologically functional in the heart, we performed dose-response studies assessing changes in $[Ca^{2+}]_i$ in response to the TRPA1 agonist, AITC or the TRPV1 agonist, capsaicin in freshly isolated CMs (Figs. 5 and 6). Real-time calcium measurements

revealed transient rises in $[Ca^{2+}]_I$ in WT CMs when treated with AITC (100 μM; Fig. 5A) or capsaicin (100 nM; Fig. 5B). The AITC- and capsaicin-induced transient rises in $[Ca^{2+}]_i$ were absent in CMs obtained from TRPA1$^{-/-}$ or TRPV1$^{-/-}$, respectively (Fig. 5C–D). CMs from all 3 groups of mice were exposed to potassium chloride (KCl; 35 mM) subsequent to agonist activation to confirm cell viability and adequate fura-2AM loading. -Similarly,
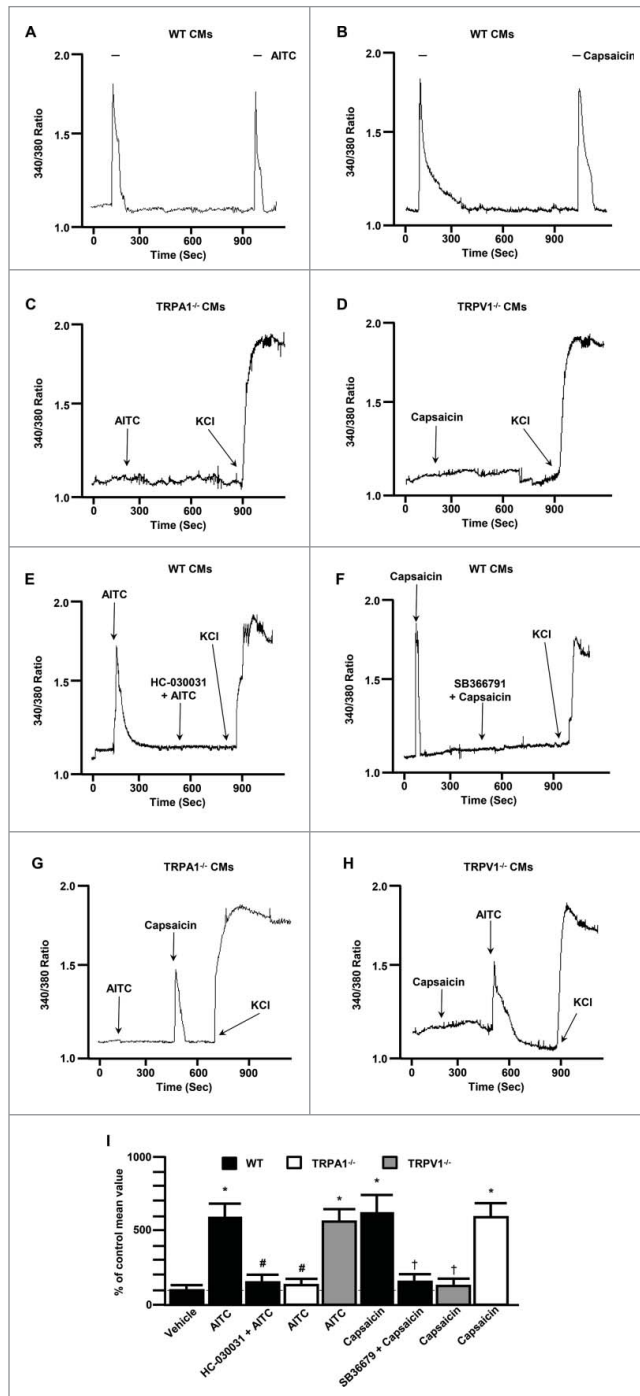
pharmacological studies indicate that the transient rises in $[Ca^{2+}]_i$ elicited via AITC and capsaicin were eliminated in WT CMs pretreated with TRPA1 antagonist, HC-030031 (500 nM; Fig. 5E) or the TRPV1 antagonist SB366791 (10 μM; Fig. 5F), respectively. Moreover, capsaicin and AITC induced transient rises in $[Ca^{2+}]_I$ in CMs obtained from TRPA1$^{-/-}$ and TRPV1$^{-/-}$ mice, respectively (Fig. 5G and 5H). Summarized data illustrating the effects of AITC or capsaicin on transient rises in $[Ca^{2+}]_i$ in CMs pretreated with pharmacological inhibitors of the channels or in CMs obtained from TRPA1$^{-/-}$ and TRPV1$^{-/-}$ mice are depicted in Figure 5G. Finally, we assessed the dose-dependency of AITC and capsaicin to elicit increases in $[Ca^{2+}]_i$ as well as the dose-dependent effects of the specific TRPA1 and TRPV1 antagonists to block the responses to AITC or capsaicin in CMs (Fig. 6). These experiments were performed using a 96 well plate fluorescent Ca^{2+} assay kit where cells in each well could be stimulated with only one dose of the agonist and/or inhibitor prior to the measurement. This was done in order to circumvent the potential for repetitive stimulation of the TRPA1 or TRPV1 channels to desensitize. Summarized data depicting the dose-dependent effect of AITC or capsaicin on $[Ca^{2+}]_i$ in CM obtained from WT and TRPA1-/- or TRPV1-/- mice are depicted in Figure 6A–B. Summarized data depicting the dose-dependent effect of the TRPA1 antagonist, HC-030031 or the TRPV1 antagonist, SB366791 on

Figure 5. Representative traces depicting the effect of TRPA1 agonist stimulation with AITC (100 μM; 10 second exposure) or TRPV1 agonist stimulation with capsaicin (100 nM; 10 second exposure) on $[Ca^{2+}]_i$ in freshly isolated CMs obtained from WT mice ((A)and B, respectively) as well as in CM's obtained from TRPA1$^{-/-}$ or TRPV1$^{-/-}$ mice ((C) and D, respectively). Representative traces depicting the effect pre-treatment with the TRPA1 antagonist, AITC HC-030031 (500 nM) or the TRPV1 antagonist, SB366791 (10 μM) on AITC- or capsaicin-induced transient rises in $[Ca^{2+}]_i$ in CMs obtained from WT mice ((E) and F, respectively). Representative traces depicting the effect of AITC or capsaicin on CMs obtained from TRPA1$^{-/-}$ and TRPV1$^{-/-}$ mice ((G) and H, respectively). CMs were treated with potassium chloride (KCl) where indicated. Summarized data for A-H (I). Data are expressed as a percent of the response observed in vehicle-treated CMs (% of control mean value $\pm$ SEM). n = experiments performed in CMs obtained from 6 separate mice. *$P < 0.05$ compared to vehicle-treated cells (ethanol). #$P < 0.05$ compared to AITC-treated WT CMs. †$P < 0.05$ compared to capsaicin-treated WT CMs. Statistical analysis performed using one way analysis of variance and the Bonferroni *post hoc* test.
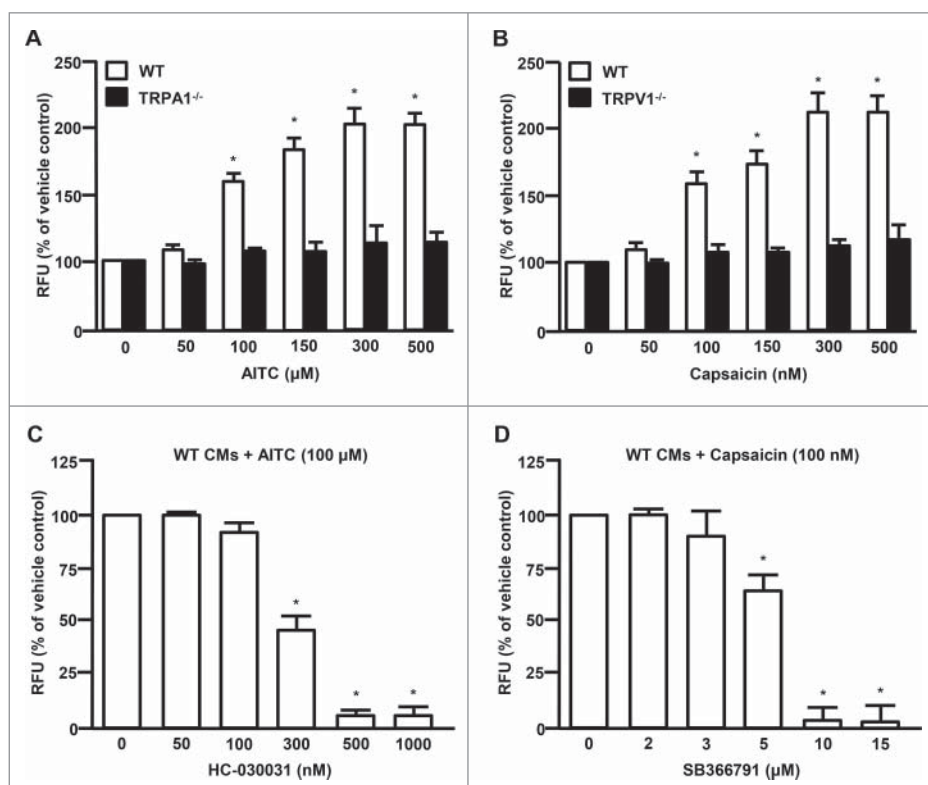
Figure 6. Summarized data depicting the dose-dependent effect of AITC or capsaicin on $[Ca^{2+}]_i$ in CMs obtained from WT, TRPA1$^{-/-}$ or TRPV1$^{-/-}$ mice ((A) and (B) respectively). Responses to ethanol alone (vehicle control) were normalized to 100% and considered the control response. Summarized data depicting the dose-dependent effect of the TRPA1 antagonist, HC-030031 or the TRPV1 antagonist, SB366791 on AITC- (100 μM) or capsaicin- (100 nM) induced increases in $[Ca^{2+}]_i$. ((C)and (D)respectively). Responses to the AITC alone (100 μM) were normalized to 100% and considered the control response. n = experiments performed in CMs obtained from 6 separate mice. $^*P < 0.05$ compared to vehicle treated (ethanol) control. Statistical analysis performed using one way analysis of variance and the Bonferroni *post hoc* test.

AITC-induced or capsaicin-induced increases in $[Ca^{2+}]_i$, respectively, are depicted in Figure 6C–D.

Discussion

To our knowledge, this is the first study to thoroughly characterize the ultrastructural localization and functional expression profiles of TRPA1 and TRPV1 ion channels in adult mouse CMs. The immunodetection, ultrastructural localization and functionality of TRPA1 channels at the protein level in cardiac muscle has not been previously reported. Although immunodetectable TRPV1 has previously been identified in mouse hearts[16,19] and appears to be located on the epicardial surface as well as in blood vessels and perivascular nerves,[19] the precise ultrastructural location of TRPV1 channels in the hearts as well as a detailed pharmacological profile of the channel has yet to be established in adult mouse CMs. The major findings of the current study are that both TRPA1 and TRPV1 are co-expressed in the adult mouse heart throughout the epicardium, myocardium as well as endocardium, and both channels appear to co-localize at the costameres, z-disc and intercalated discs in isolated CMs. Moreover, both TRPA1 and TRPV1 channels are functional in isolated CMs since both channels respond to selective agonist stimulation with a transient increase in $[Ca^{2+}]_i$ in a dose-dependent manner, an effect that is dose-dependently attenuated with specific channel antagonists and is absent all together in CMs obtained from TRPA1$^{-/-}$ and TRPV1$^{-/-}$ mice.

TRPA1 and TRPV1 expression in cardiac tissue

The superfamily of TRP ion channels play important roles in the physiology of the cardiovascular system by regulating fundamental cell functions such as contraction, relaxation, proliferation, differentiation and cell death,[11] but also play an important role in the pathophysiology of many diseases in the cardiovascular system.[22-25] Although the expression, ultrastructural localization and physiological/pathophysiological role

(s) for TRPA1 ion channels in myocardial tissue has yet to be determined, the expression of TRPV1 channels in cardiac muscle and their role in physiological/ pathophysiological processes in the heart have recently been reported and are rapidly emerging as key players in a myriad of cellular and molecular events related to cardiac diseases. For example. several studies have demonstrated the presence of TRPV1 in cardiac muscle and an important role for the channel in mediating myocardial protection from ischemic injury.[19,26-28] In contrast, evidence also exists for TRPV1 channels playing a role in the development of the pathophysiology of cardiac hypertrophy and heart failure[18,29] whereas another study indicated TRPV1 activation attenuates high-salt diet-induced cardiac hypertrophy and fibrosis.[16] Limited information is available describing where in the heart TRPV1 channels are expressed, which specific cell types are involved (myocytes, fibroblasts, vasculature, etc) and where is the precise ultrastructural location of the channel in cells where it is expressed. Previous studies by our laboratory have identified that the sensitivity of TRPV1 channels to agonist activation can be modulated by TRPA1 channel agonists indicating crosstalk/regulation between the channels that may be vital for altering cellular responses to noxious stimuli in sensory neurons.[20,21,30] Because TRPA1 protein has not yet been reported in cardiac muscle, but plays an important regulatory role in sensory neurons when co-expressed with TRPV1, our objectives were to identify the extent to which TRPA1 is co-expressed with TRPV1 in cardiac muscle and determine their precise ultrastructural locations within the CM. Identifying the localization of these channels could provide important fundamental insight and clarification into their roles in physiological and pathophysiological consequences.

Our studies clearly indicate that both TRPA1 and TRPV1 are expressed throughout the heart and appear to localize at the costameres, z-discs and intercalated discs in adult mouse CMs. Costameres are critically important cytoskeletal structures demonstrated to have significant roles in mechanosensation and bidirectional signal transduction in CMs.[31,32] Functionally, they are similar to focal adhesion complexes but they are found in register with Z-discs and circumferentially couple the cardiac myofibrils to the sarcolemma. The positioning of costameres within the ultrastructure of the CM eludes to their vast ability to

modulate physiological and pathophysiological events in cardiac tissue. Furthermore, Z-discs are commonly regarded as "internal costameres," by which they share similar functional roles in CM biochemical signal transduction; each are implicated in sensing mechanical stress and subsequent conversion of stress signals into alterations of protein synthesis, cell-cell communication, protein assembly within the sarcomere and ion channel function, among others.[33-35] The exact mechanisms by which mechanical stimuli are converted into biochemical responses remain elusive, however, mechanosensitive ion channels have been implicated as potential players by which they mediate mechanisms that occur between the cytoskeleton and the sarcolemma.[36] Although the roles of TRPA1 and TRPV1 channels play in mediating intracellular signaling pathways and molecular mechanisms within cardiac tissue remains elusive, these channels are understood to be mechanosensitive, signal transducers in other cell types throughout the body[1,23] – characteristics which may elude to which intracellular and intercellular events the channels play a role in regulating within CMs. Since TRPA1 and TRPV1 have been demonstrated to serve roles in mechanosensation in tissues throughout the body,[37-39] we speculate they will serve a similar role in ventricular CMs, by which they can sense external stimuli and transmit that signal internally. Furthermore, the localization of TRPA1 and TRPV1 at the region of the presumed intercalated discs suggests the ion channels may serve a role in cell-cell adhesion or the propagation of chemical and electrical signals through the network of the lattice-like cardiac tissue.

Even though costameres are generally investigated in regards to their ability to transmit contractile forces from the inside of CMs to neighboring tissues, as well as converting forces generated in the extracellular matrix to intracellular biochemical signals, costameres and Z-discs are also known to be muscle cell signaling "hot-spots".[35] Although there is a paucity of information underlying the signaling pathways elicited via TRPA1 and/or TRPV1 activation in CMs, the ion channels have been demonstrated to induce a myriad of intracellular signaling events upon stimulation in other cell types.[21,30,38] Indeed, mechanistically delineating intracellular signaling events elicited via TRPA1 and TRPV1 stimulation and the potential role for cross-regulation of the channels in mediating cellular events in cardiac muscle, particularly in mediating

myocardial protection, is of great clinical significance and will be the focus of future investigations.

Regulation of cardiac function by TRP channels is typically attributed to TRP-channel-expressing cardiac nerve afferents innervating the heart tissue, itself.[40,41] Consequentially, TRP channel physiological and pathophysiological functionality within cardiac tissue/CMs has yet to be fully elucidated. As noted earlier, a previous study indicated that TRPV1 appeared to localize predominantly to the epicardial layer of the heart[19]; however, results included within this investigation indicate that both TRPA1 and TRPV1 are expressed throughout the 3 layers (endocardium, myocardium, epicardium) of cardiac tissue. Although previous investigations have demonstrated the role of TRPV1 in hypertrophy and heart failure,[18,29] the extent to which TRPA1 and TRPV1 regulate basal cardiac function remains elusive. Furthermore, although TRPV1 has been extensively investigated in regards to its role in myocardial protection following ischemia,[19,26-28] further studies are required in order to precisely determine how TRPA1 and TRPV1 channel function is altered in pathological conditions.

TRPA1 and TRPV1 stimulation elicits calcium influx in CMs

As stated previously, TRPA1 and TRPV1 are non-selective cation channels that tend to show high permeability to calcium.[1] Although we demonstrate co-expression and co-localization of both TRPA1 and TRPV1 in CMs, we next sought to determine whether the channels are functional and explore their sensitivity to agonist activation which should result in transient increases in $[Ca^{2+}]_i$ in CMs. Our studies indicate that the selective agonists for TRPA1 (AITC) or TRPV1 (capsaicin) channels causes a dose-dependent transient rise in $[Ca^{2+}]_i$. Moreover, this effect was absent in CMs obtained from TRPA1$^{-/-}$ and TRPV1$^{-/-}$ mice indicating that AITC and capsaicin selectively stimulate calcium influx through functional TRPA1 and TRPV1, respectively. Similarly, the agonist-induced transient rise in $[Ca^{2+}]_i$ was dose-dependently attenuated when CMs obtained from WT mice were pretreated with selective antagonists of TRPA1 (HC-030031) or TRPV1 (SB366791) prior to agonist stimulation. These transient increases in $[Ca^{2+}]_i$ are similar to our previous findings in sensory neurons and indicate functional gating of the channels in

response to the agonists as well as pharmacological sensitivity to well established antagonists of each channel. A dose-dependent increase in $[Ca^{2+}]_i$ was previously observed in a cultured cardiac cell line (H9c2 cells), however the response to capsaicin was a sustained elevation in $[Ca^{2+}]_i$ which did not return to baseline suggesting that the TRPV1 channels in this cell line may not be gating properly.[16]

Calcium regulation in CMs partially dictates inotropic, chronotropic and lusitropic properties and the resulting cellular energetics within cardiac tissue. Although TRP channel-mediated calcium entry has been shown to induce intracellular signaling cascades in several other cell types,[42-44] as well as induce fibroblast proliferation and differentiation leading to various forms of arrhythmia, hypertrophy or heart failure,[45-47] the extent to which TRPA1 and TRPV1 modulate these effects in CMs remains to be determined and will be the focus of future investigations. Taken together with the polymodal activation characteristics of TRP channels, we speculate that TRPA1 and TRPV1 may have diverse functions in cardiac physiology and pathophysiology. However, since TRP channels are able to integrate and initiate signaling events via calcium entry and consequential membrane depolarization, it is feasible to hypothesize a role for these channels in mediating cellular functions such as contraction, relaxation, myogenic regulation (perhaps due to mechanosensation) and cell death in the heart.

Summary and conclusions

Due to the paucity of information regarding the functional expression and localization of TRPA1 and TRPV1 in cardiac tissue, this investigation was designed to examine expression patterns of the ion channels in freshly isolated CMs and to begin delineating the physiological functions of the channels in response to agonist stimulation. Overall, our current findings are consistent with previous reports of TRPV1 expression in the heart,[11,19,48] but the reporting of TRPA1 at the protein level in CMs is novel in nature. Furthermore, we demonstrate that TRPA1 and TRPV1 are expressed throughout the different layers of the heart and they colocalize at the intercalated discs, but are most heavily concentrated at the Z-discs and costameres within the CM cytoskeleton. The localization of TRPA1 and TRPV1 in CMs have prompted several hypotheses. First, the Z-disc is the

site of localization for many proteins, which indicate that the ion channels may share similar signaling pathways and/or are involved in direct physical interactions with other structures located therein. Secondly, CMs have stress-strain sensors embedded at several locations, including the Z-disc, costameres and intercalated discs; this suggests a potential role for the receptors in mediating mechanotransduction.[49] Lastly, the localization of the channels at the intercalated discs could be correlated with the presence of proteins which mediate calcium-dependent cell-to-cell adhesion, such as N-cadherin.[50,51] Moreover, stimulation of TRPA1 and TRPV1 in freshly isolated CMs induces dose-dependent, transient rises in $[Ca^{2+}]_I$ – effects which can be dose-dependently eliminated through the use of selective channel antagonists. In order to identify the myriad of events likely to be modulated by the presence and activation of TRPA1 and TRPV1 in cardiac tissue, future studies are required to further elucidate whether the channels communicate (either directly or indirectly) and the extent to which they mediate physiological events. In conclusion, the results included herein provide a foundation for proceeding investigations designed to determine the precise physiological functions of TRPA1 and TRPV1 in cardiac tissue. Delineating the signal transduction pathways and molecular mechanisms to which they are involved will provide fundamental insight into uncovering novel information regarding the regulation of TRPA1- and TRPV1-mediated physiological and pathophysiological events in cardiac tissue.

Materials and methods

Animal model

Four-month-old male C57BL/6 mice (n = 6/group) were used and maintained in accordance with the *Guide for the Care and Use of Laboratory Animals* (NIH). All animals were housed at the Kent State University animal care facility (Kent, OH), which is accredited by the American Association for Accreditation of Laboratory Animal Care.

Isolation of CMs

Murine hearts were excised and transferred to a Langendorff apparatus for C) isolation, as previously described.[52] In brief, mice were sacrificed via cervical dislocation and hearts were rapidly excised then placed into a dish containing perfusion buffer. After the aorta was cannulated and blood was flushed, the hearts were subjected to retrograde perfusion at 37°C and pH 7.4 with a modified Krebs-Henseleit buffer (in mM: 120.4 NaCl, 4.8 KCl, 0.6 KH_2PO_4, 0.6 Na_2HPO_4, 1.2 $MgSO_4$-7H_8O, 10 Na-HEPES, 4.6 $NaHCO_3$, 30 taurine, 10 B.M. and 5.5 glucose). The calcium-free buffer was sterile-filtered and paced with a peristaltic pump (Masterflex) to begin retrograde perfusion of the heart at a rate of 4 mL/min. After perfusion for 4 minutes, the same solution containing collagenase type II (300 U/mg, Worthington Biochemical) perfused the heart for an additional 8 minutes until the heart became soft. The left ventricles were removed, minced, then triturated in Krebs-Henseleit buffer containing fetal bovine serum. The resulting cellular digest was washed and resuspended in HEPES-buffered saline (in mM: 118 NaCl, 4.8 KCl, 0.6 KH_2PO_4, 4.6 $NaHCO_3$, 0.6 NaH_2PO_4, 5.5 glucose, pH 7.4) at 23°C. CM yield was typically ~80–90%. CMs were then either subjected to immunoblotting, immunocytochemistry, or slow calcium reintroduction ([1.23 mM]) and subsequent $[Ca^{2+}]_i$ measurements.

F-11 cell transfection with TRPV1 or TRPA1

F-11 cell transfection was carried out as previously described.[30] Cultured F-11 cells (hybridoma cell line) were transfected with TRPA1 or TRPV1 cDNA via electroporation using a Neon Transfection System (Invitrogen). In brief, cultured F-11 cells were harvested and washed with phosphate-buffered saline without calcium or magnesium. The cells were then resuspended in electrolytic buffer, where TRPA1 and TRPV1 cDNA was then added. Using a pulse voltage of 1500 V, a pulse width of 35 msec, and a pulse number of 2, electroporation was then performed. The cells were then suspended in Dulbecco's Modified Eagle's Medium supplemented with 10% fetal bovine serum at 37°C. The cells were used to demonstrate the presence of TRPA1 or TRPV1 in immunoblot analysis.

Preparation of cell lysates and immunoblot analysis

Immunoblot analysis was performed as previously described.[53] CMs were homogenized in a lysis buffer (in mM: 25 Tris-HCl, 150 NaCl, 1% NP-40, 1% sodium deoxycholate, 0.1% SDS, pH 7.6) and protein concentration was assessed using the Bradford method (Bradford, 1976). All samples were adjusted

to 2 mg/mL protein concentration in sample buffer. Samples containing equal amount of protein lysates (50 μg) were boiled then subjected to SDS-PAGE on a 4–15% precast polyacrylamide gels, (Bio-Rad) through the use of a minigel apparatus, which were then transferred to nitrocellulose membranes. Nonspecific binding was blocked with 5% nonfat milk in Tris-buffered saline solution (0.1% [vol/vol] Tween-20 in 20 mM Tris base, 137 mM NaCl, pH 7.6 containing 3% bovine serum albumin) for 45 minutes at room temperature. Polyclonal antibodies against TRPA1 (Novus Biologicals) and TRPV1 (Santa Cruz Biotechnology) were diluted 1:500 in Tris-buffered saline containing 5% nonfat milk and incubated at 4°C overnight. After washing in Tris-buffered saline, membranes were incubated for 1 h at room temperature with horseradish-peroxidase linked secondary antibody (goat anti-mouse and goat anti-rabbit) diluted 1:5000 in Tris-buffered saline with 5% nonfat milk. Antibody detection was conducted via enhanced chemiluminescence with an ImageQuant LAS 4000 Mini (General Electric) and immunoreactivity was quantified by scanning densitometry and analyzed using ImageJ software (NIH).

Immunocytochemistry

Immunocytochemistry techniques were carried out as previously described.[53] CMs were allowed to adhere to laminin-coated coverslips (20μg/mL) at 37°C for 2 h and subsequently fixed in a 1:1 acetone/methanol solution for 30 minutes. After washing with phosphate-buffered saline, cells were blocked before addition of primary antibodies. After blocking has occurred, CMs were double stained with combinations of the following primary antibodies: anti-α-actinin, anti-vinculin (Upstate Biotechnology, Lake Placid, NY), rabbit anti-TRPA1 and/or mouse anti-TRPV1. Alexa Fluor 488-conjugated donkey anti-rabbit and Alexa Fluor 568-conjugated donkey anti-mouse (Life Technologies) were used as secondary antibodies. Negative controls included CMs incubated with a single primary antibody and both secondary antibodies, as well as CMs incubated with secondary antibodies alone. Images were acquired using an Olympus Fluoview 100 confocal laser scanning microscope with an X63 objective lens.All images were acquired utilizing a 60X objective with a gain setting of 500 V and laser excitation wavelengths of 488 nm (multi-line Ar, 8.0%

full power, BA505-525 filter) and 543 nm (HeNe, 12.0% full power, BA560-660 filter).

Immunohistochemistry

Hearts were rapidly excised and placed immediately in 4% paraformaldehyde (PFA) and incubated overnight at 4°C. Samples were rinsed and then incubated in 4°C overnight in increasing concentrations of sucrose (10, 15, 30%). Hearts were then frozen into Tissue-Tek OCT tissue-freezing medium (Sakura Finetek) and prepared for sectioning. Transverse cryosections were taken at 30 μM using a Leica cryostat and mounted on super frost plus coated glass slides. The slides were blocked and stained as previously described[54] using the same antibodies that were applied in the immunocytochemistry experiments, including DAPI. Negative controls included TRPA1$^{-/-}$ or TRPV1$^{-/-}$ heart sections stained with TRPA1 and TRPV1 antibodies, respectively, and WT heart sections incubated with secondary antibodies in the absence of a primary. Slides were visualized using a laser scanning confocal microscope with an oil immersion lens at 10X and 60X. All images were acquired with a gain setting of 500 V and laser excitation wavelengths of 488 nm (8.0% full power, BA505-525 filter) and 543 nm (12.0% full power, BA560-660 filter). Z-stack images were taken at several levels of cardiac myofibers to assess the physical depth of immunostaining and to confirm the localization of TRPA1 and TRPV1 ion channels at the costameres and Z-discs.

$[Ca^{2+}]_i$ measurements

$[Ca^{2+}]_i$ measurements were performed as previously described.[55] For real-time intracellular calcium measurements, CMs were allowed to adhere to laminin-coated cover slips and incubated at room temperature for 30 min with fura-2 acetoxy methylester (fura-2/AM; 2 μM) in HEPES-buffered saline (in mM: 118 NaCl, 4.8 KCl, 1.23 CaCl$_2$, 0.6 KH$_2$PO$_4$, 4.6 NaHCO$_3$, 0.6 NaH$_2$PO$_4$, 5.5 glucose, pH 7.4). Coverslips containing the fura-2-loaded CMs were then mounted on the stage of an Olympus IX-81 inverted fluorescence microscope (Olympus America). CMs were superfused continuously with HEPES-buffered saline at a flow rate of 2 mL/min and compounds (agonists, antagonists) were delivered for ~10 sec with a 10 min wash period between subsequent treatments. Potassium chloride

(KCl; 35 mM) was utilized to confirm that the CMs are polarized and respond to KCl-triggered depolarization leading to the activation of the voltage-gated L-type Ca^{2+} channels. $[Ca^{2+}]_I$ measurements were simultaneously recorded on individual cells using the fluorescence imaging system and Easy Ratio Pro software (Photon Technology International) equipped with a multiwavelength spectrofluorometer (Deltascan RFK6002) and a QuantEM 512SC electron multiplying camera (Photometrics). Images and real-time calcium tracing data were acquired using an alternating excitation wavelength protocol (340, 380 nm/20 Hz) and emission wavelength of 510 nm. Background fluorescence was automatically corrected for the experiments using Easy Ratio Pro. The ratio of the 2 intensities was used to measure changes in $[Ca^{2+}]_I$ due to the fact that calibration of the system relies upon a number of assumptions. Dose response curves to agonists alone or agonist in the presence of increasing concentrations of antagonists were performed utilizing a fluorescent calcium assay kit (Molecular Probes) and a dual-wavelength multi-mode detector (DTX 880, Beckamn Coulter) with excitation and emission wavelengths set at 494 and 516 nm, respectively. CMs were centrifuged and resuspended in assay buffer (1X HBSS, 20 mM HEPES) and pipetted into a 96-well plate and then incubated at 37°C for ∼1 h to allow the cells to settle. A dye mix (containing Fluo-4 NW and probenecid) was subsequently added to the wells and incubated for 30 min at 37°C and then for an additional 30 min at room temperature. Increasing concentrations of AITC or capsaicin were aliquoted into each of the wells (10 min prior to measurement) to obtain dose-response curves for agonist-induced increases in $[Ca^{2+}]_i$. Similarly, dose response curves following a 10 min pre-treatment of increasing concentrations of the antagonists prior to addition of a maximal dose of channel agoinst were also performed. Results were quantified and are expressed as mean ± SEM.

Statistical analysis

$[Ca^{2+}]_I$ imaging experimental protocols were repeated with a minimum of 6 separate coverslips containing CMs from the respective groups. Results from each coverslips were averaged so each coverslip of CMs were equally weighted in calculations. The Shapiro-Wilk normality test was used to examine the Gaussian distribution. Comparisons between the groups were made utilizing repeated-measures one-way ANOVA and Bonferroni post hoc text (p < 0.05). All results are expressed as mean ± SEM. Error bars in the figures signify the variability of peak $[Ca^{2+}]_I$ intensities in calcium imaging experiments or in the calcium assay as noted in the legends. Statistical analysis was carried out using Sigma Plot 11.0 software (Systat Software).

Abbreviations

AITC　　allyl isothiocyanate
$[Ca^{2+}]_I$　intracellular free calcium concentration
CM　　　adult mouse ventricular cardiomyocyte
TRPA1　transient receptor potential ankyrin channel subtype-1
TRPV1　transient receptor potential vanilloid channel subtype-1

Disclosure of potential conflicts of interest

No potential conflicts of interest were disclosed.

Author contributions

SA, PS, IB and DD participated in research design and data analysis. SA and PS conducted the experiments. SA, PS, IB and DD wrote or contributed to the writing of the manuscript.

References

[1] Fernandes ES, Fernandes MA, Keeble JE. The functions of TRPA1 and TRPV1: moving away from sensory nerves. Br J Pharmacol 2011; 166:510-21; http://dx.doi.org/10.1111/j.1476-5381.2012.01851.x

[2] Patil MJ, Jeske NA, Akopian AN. Transient receptor potential V1 regulates activation and modulation of transient receptor potential A1 by Ca²⁺. Neuroscience 2010; 171:1109-19; PMID:20884333; http://dx.doi.org/10.1016/j.neuroscience.2010.09.031

[3] Staruschenko A, Jeske N, Akopian A. Contribution of TRPV1-TRPA1 interaction to the single-channel properties of the TRPA1 channel. J Biol Chem 2010; 285: 15167-77; PMID:20231274; http://dx.doi.org/10.1074/jbc.M110.106153

[4] Horvath A, Tekus V, Boros M, Pozsgai G, Botz B, Borbely E, Szolcsanyi J, Pinter E, Helyes Z. Transient receptor potential ankyrin 1 (TRPA1) receptor is involved in chronic arthritis: in vivo study using TRPA1-deficient mice. Arthritis Res Ther 2016; 18(1):6; PMID:26746673; http://dx.doi.org/10.1186/s13075-015-0904-y

[5] Meseguer V, Alpizar YA, Luis E, Tajada S, Denlinger B, Fajardo O, Manenschjin JA, Fernandez-Pena C, Talavera A, Kichko T, et al. TRPA1 channels mediate acute neurogenic inflammation and pain produced by bacterial endotoxins. Nat Commun 2014; 5:3125.

[6] Fusi C, Materazzi S, Benemei S, Coppi E, Trevisan G, Marone IM, Minocci D, De Logu F, Tuccinardi T, Di Tommaso MR, Susini T, Moneti G, Pieraccini G, Geppetti P, Nassini R. Steroidal and non-steroidal third-generation aromatase inhibitors induce pain-like symptoms via TRPA1. Nat Commun 2014; 5:5736.

[7] Schwartz ES, La JH, Scheff NN, Davis BM, Albers KM, Gebhart GF. TRPV1 and TRPA1 antagonists prevent the transition of acute to chronic inflammation and pain in chronic pancreatitis. J Neurosci 2013; 33:5603-11; PMID:23536075; http://dx.doi.org/10.1523/JNEUROSCI.1806-12.2013

[8] Caterina MJ, Schumacher MA, Tominaga M, Rosen TA, Levine JD, Julius D. The capsaicin receptor: a heat-activated ion channel in the pain pathway. Nature 1997; 389(6653):816-24; PMID:9349813; http://dx.doi.org/10.1038/39807

[9] Caterina MJ, Julius D. The vanilloid receptor: A molecular gateway to the pain pathway. Annu Rev Neurosci 2001; 24:487-517; http://dx.doi.org/10.1146/annurev.neuro.24.1.487

[10] Story G, Peier A, Reeve A, Eid S, Mosbacher J, Hricik T, Earley T, Hergarden A, Andersson D, Hwang S, McIntyre P, Jegla T, Bevan S, Patapoutian A. ANKTM1, a TRP-like channel expressed in nociceptive neurons, is activated by cold temperature. Cell 2003; 112:819-29; PMID:12654248; http://dx.doi.org/10.1016/S0092-8674(03)00158-2

[11] Yue Z, Zie J, Yu AS, Stock J, Du J, Yue L. Role of TRP channels in the cardiovascular system. Am J Physiol Heart Circ Physiol 2015; 308(3):H157-82; PMID:25416190; http://dx.doi.org/10.1152/ajpheart.00457.2014

[12] Pazienza V, Pomara C, Appello F, Alogero R, Arrara M, Azzoccoli G, Inciguerra M. The TRPA1 channel is a cardiac target of mIGF-1/SIRT1 signaling. Am J Physiol Heart Circ Physiol 2014; 307:H939-H944; PMID:25108014; http://dx.doi.org/10.1152/ajpheart.00150.2014

[13] Oguri G, Nakajima T, Yamamoto Y, Takano N, Tanaka T, Kikuchi H, Morita T, Nakamura F, Yamasoba T, Komuro I. Effects of methylglyoxal on human cardiac fibroblast: roles of transient receptor potential ankyrin 1 (TRPA1) channels. Am J Physiol Heart Circ Physiol 2014; 307:H1339-H1352; PMID:25172898; http://dx.doi.org/10.1152/ajpheart.01021.2013

[14] Lu MJ, Chen YS, Huang HS, Ma MC. Hypoxic preconditioning protects rat hearts against ischemia-reperfusion injury via the arachidonate 12-lipoxygenase/transient receptor potential vanilloid 1 pathway. Basic Res Cardiol 2014; 109 (4):414; http://dx.doi.org/10.1007/s00395-014-0414-0

[15] Lang H, Li Q, Yu H, Li P, Lu Z, Xiong S, Yang T, Zhao Y, Huang X, Gao P, Zhang H, Shang Q, Liu D, Zhu Z. Activation of TRPV1 attenuates high salt-induced cardiac hypertrophy through improvement of mitochondrial function. Br J Pharmacol 2015; 172(23):5548-58; PMID:25339153

[16] Gao F, Liang Y, Wang X, Lu Z, Li L, Zhu S, Liu D, Yan Z, Zhu Z. TRPV1 Activation Attenuates High-Salt Diet-Induced Cardiac Hypertrophy and Fibrosis through PPAR-d Upregulation. PPAR Res 2014; 2014:491963; PMID:25152753

[17] Wang Q, Ma S, Li D, Zhang Y, Tang B, Qui C, Yang Y, Yang D. Dietary capsaicin ameliorates pressure overload-induced cardiac hypertrophy and fibrosis through the transient receptor potential vanilloid type 1. Am J Hypertens 2014; 27:1521-9; PMID:24858305; http://dx.doi.org/10.1093/ajh/hpu068

[18] Buckley CL, Stokes AJ. Mice lacking functional TRPV1 are protected from pressure overload cardiac hypertrophy. Channels 2011; 5:367-74; PMID:21814047; http://dx.doi.org/10.4161/chan.5.4.17083

[19] Zhong B, Wang DH. Protease-activated receptor 2-mediated protection of myocardial ischemia-reperfusion injury: role of transient receptor potential vanilloid receptors. Am J Physiol Regul Integr Comp Physiol 2009; 297 (6):R1681-R1690; PMID:19812353; http://dx.doi.org/10.1152/ajpregu.90746.2008

[20] Wickley PJ, Yuge R, Russell MS, Zhang H, Sulak M, Damron DS. Propofol Modulates Agonist-Induced Transient Receptor Potential Vanilloid Subtype-1 Receptor De-sensitization via a Protein Kinase C epsilon-Dependent Pathway in Mouse Dorsal Root Ganglion Sensory Neurons. Anesthesiology 2010; 113:833-44; PMID:20808213; http://dx.doi.org/10.1097/ALN.0b013e3181eaa9a0

[21] Zhang H, Wickley PJ, Sinha S, Bratz IN, Damron DS. Propofol Restores Transient Receptor Potential Vanilloid Receptor Subtype-1 Sensitivity via Activation of Transient Receptor Potential Ankyrin Receptor Subtype-1 in Sensory Neurons. Anesthesiology 2011; 114:1169-79; PMID:21364461; http://dx.doi.org/10.1097/ALN.0b013e31820dee67

[22] Inoue R, Jensen LJ, Shi J, Morita H, Nishida M, Honda A, Ito Y. Transient Receptor Potential Chan-

nels in Cardiovascular Function and Disease. Circ Res 2006; 99:119-31; PMID:16857972; http://dx.doi.org/10.1161/01.RES.0000233356.10630.8a

[23] Inoue R, Jian Z, Kawarabayashi Y. Mechanosensitive TRP channels in cardiovascular pathophysiology. Pharmacol Ther 2009; 123(3):371-85; PMID:19501617; http://dx.doi.org/10.1016/j.pharmthera.2009.05.009

[24] Vennekens R. Emerging concepts for the role of TRP channels in the cardiovascular system. J Physiol 2011; 589(Pt 7):1527-34; PMID:21173080http://dx.doi.org/10.1113/jphysiol.2010.202077

[25] Watanabe H, Murakami M, Ohba T, Takahashi Y, Ito H. TRP channel and cardiovascular disease. Pharmacol Ther 2008; 118:337-51

[26] Zhong B, Wang DH. TRPV1 gene knockout impairs preconditioning protection against myocardial injury in isolated perfused hearts in mice. Am J Physiol Heart Circ Physiol 2007; 293:H1791-H1798; PMID:17586621; http://dx.doi.org/10.1152/ajpheart.00169.2007

[27] Sexton A, McDonald M, Cayla C, Thiemermann C, Ahluwalia A. Twelve-Lipoxygenase-derived eicosanoids protect against myocardial ischemia/reperfusion injury via activation of neuronal TRPV1. FASEB J 2007; 21:2695-703; PMID:17470568; http://dx.doi.org/10.1096/fj.06-7828com

[28] Wang L, Wang DH. TRPV1 Gene Knockout Impairs Postischemic Recovery in Isolated Perfused Heart in Mice. Circulation 2005; 112:3617-23; PMID:16314376; http://dx.doi.org/10.1161/CIRCULATIONAHA.105.556274

[29] Horton JS, Buckley CL, Stokes AJ. Successful TRPV1 antagonist treatment for cardiac hypertrophy and heart failure in mice. Channels 2013; 7:17-22; PMID:23221478; http://dx.doi.org/10.4161/chan.23006

[30] Sinharoy P, Zhang H, Sinha S, Prudner BC, Bratz IN, Damron DS. Propofol restores TRPV1 sensitivity via a TRPA1-, nitric oxide synthase-dependent activation of PKC epsilon. Pharmacol Res Perspect 2015; 3(4):e00153; PMID:26171233; http://dx.doi.org/10.1002/prp2.153

[31] Knoll R. A role for membrane shape and information processing in cardiac physiology. Pflug Arch Eur J Phy 2015; 467:167-73; http://dx.doi.org/10.1007/s00424-014-1575-2

[32] Jaka O, Casas-Fraile L, Lopez De Munain A, Saenz A. Costamere proteins and their involvement in myopathic processes. Expert Rev Mol Med 2015; 17:e12; PMID:26088790; http://dx.doi.org/10.1017/erm.2015.9

[33] Vasioukhin V, Bauer C, Yin M, Fuchs E. Directed actin polymerization is the driving force for epithelial dependent cell-cell adhesion. Cell 2000; 100:209-19; PMID:10660044; http://dx.doi.org/10.1016/S0092-8674(00)81559-7

[34] Capetanaki Y, Bloch RJ, Kouloumenta A, Mavroidis M, Psarras S. Muscle intermediate filaments and their links to membranes and membranous organelles. Exp Cell Res 2007; 313:2063-76; PMID:17509566; http://dx.doi.org/10.1016/j.yexcr.2007.03.033

[35] Samarel AM. Costameres, focal adhesions, and cardiomyocyte mechanotransduction. Am J Physiol Heart Circ Physiol 2015; 289:H2291-H2301; http://dx.doi.org/10.1152/ajpheart.00749.2005

[36] Ervasti JM. Costameres: the Achilles' Heel of Herculean Muscle. J Biol Chem 2003; 278:13591-4; PMID:12556452; http://dx.doi.org/10.1074/jbc.R200021200

[37] Brierly SM, Castro J, Harrington AM, Hughes PA, Page AJ, Rychkov GY, Blackshaw LA. TRPA1 contributes to specific mechanically activated currents and sensory neuron mechanical hypersensitivity. J Physiol 2011; 589(Pt 14):3593.

[38] Lin CS, Lee SH, Huang HS, Chen YS, Ma MC. H2O2 generated by NADPH oxidase 4 contributes to transient receptor potential vanilloid 1-channel mediated mechanosensation in the rat kidney. Am J Physiol Renal Physiol 2015; 309:F369-F376; PMID:26136558; http://dx.doi.org/10.1152/ajprenal.00462.2014

[39] Sappington RM, Sidorova T, Ward NJ, Chakravarthy R, Ho KW, Calkins DJ. Activation of transient receptor potential vanilloid-1 (TRPV1) influences how retinal ganglion cell neurons respond to pressure-related stress. Channels (Austin) 2015; 9:102-13; PMID:25713995; http://dx.doi.org/10.1080/19336950.2015.1009272

[40] Pan H, Chen S. Sensing tissue ischemia: another new function of capsaicin receptors? Circulation 2004; 110(13):1826-31; PMID:15364816; http://dx.doi.org/10.1161/01.CIR.0000142618.20278.7A

[41] Zvara A, Bencsik P, Fodor G, Csont T, Hackler L Jr, Dux M, Furst S, Jancso G, Puskas LG, Ferdinandy P. Capsaicin-sensitive sensory neurons regulate myocardial function and gene expression pattern of rat hearts: a DNA microarray study. FASEB 2006; 20:160-2.

[42] Ambudkar IS. Calcium signalling in salivary physiology and dysfunction. J Physiol 2015; PMID:26592972

[43] Kurosaka M, Ogura Y, Funabashi T, Akema T. Involvement of Transient Receptor Potential Cation Channel Vanilloid 1 (TRPV1) in Myoblast Fusion. J Cell Physiol 2016; PMID:26892397

[44] Stueber T, Eberhardt MJ, Hadamitzky C, Jangra A, Schenk S, Dick F, Stoetzer C, Kistner K, Reeh PW, Binshtok AM, Leffler A. Quaternary Lidocaine Derivative QX-314 Activates and Permeates Human TRPV1 and TRPA1 to Produce Inhibition of Sodium Channels and Cytotoxicity. Anesthesiology 2016; 124(5):1153-656; PMID:26859646

[45] Du J, Xie J, Zhang Z, Tsujikawa H, Fusco D, Silverman D, Liang B, Yue L. TRPM7-mediated Ca^{2+} signals confer fibrogenesis in human atrial fibrillation. Circ Res 2010; 106:992-1003; PMID:20075334; http://dx.doi.org/10.1161/CIRCRESAHA.109.206771

[46] David J, Burr AR, David GF, Birnbaumer L, Molkentin JD. A TRPC6-dependent pathway for myofibroblast transdifferentiation and wound healing in vivo. Dev Cell 2012; 23:705-15; PMID:23022034; http://dx.doi.org/10.1016/j.devcel.2012.08.017

[47] Harada M, Luo X, Qi XY, Tadevosyan A, Maguy A, Ordog B, Ledoux J, Kato T, Naud P, Voigt N, et al. TRPC3-dependent fibroblast regulation in atrial fibrillation.

Circulation 2012; 126:2051-64; PMID:22992321; http://dx.doi.org/10.1161/CIRCULATIONAHA.112.121830

[48] Pei Z, Zhuang Z, Sang H, Wu Z, Meng R, He EY, Scott GI, Maris JR, Li R, Ren J. α,β-unsaturated aldehyde crotonaldehyde triggers cardiomyocyte contractile dysfunction: Role of TRPV1 and mitochondrial function. Pharmacol Res 2014; 82:40-50; PMID:24705155; http://dx.doi.org/10.1016/j.phrs.2014.03.010

[49] Hoshijima M. Mechanical stress-strain sensors embedded in cardiac cytoskeleton: Z disk, titin, and associated structures. Am J Physiol Heart Circ Physiol 2006; 290:H1313-H1325; PMID:16537787; http://dx.doi.org/10.1152/ajpheart.00816.2005

[50] Sheikh F, Ross RS, Chen J. Cell-Cell Connection to Cardiac Disease. Trends Cardiovas Med 2009; 19(6):182-90; http://dx.doi.org/10.1016/j.tcm.2009.12.001

[51] Li J. Alterations in cell adhesion proteins and cardiomyopathy. World J Cardiol 2014; 6(5):304-13; PMID:24944760

[52] O'Connell TD, Rodrigo MC, Simpson PC. Isolation and Culture of Adult Mouse Cardiac Myocytes. Methods Mol Biol 2007; 357:271-96; PMID:17172694

[53] Wickley PJ, Murray PA, Damron DS. Propofol-induced activation of protein kinase C isoforms in adult rat ventricular myocytes. Anesthesiology 2006; 104:970-7; PMID:16645449; http://dx.doi.org/10.1097/00000542-200605000-00013

[54] Russell MA, Lund LM, Haber R, McKeegan K, Cianciola N, Bond M. The intermediate filament protein, synemin, is an AKAP in the heart. Arch Biochem Biophys 2006; 456:204-15; PMID:16934740; http://dx.doi.org/10.1016/j.abb.2006.06.010

[55] Kanaya N, Gable B, Murray PA, Damron DS. Propofol increases phosphorylation of troponin I and myosin light chain 2 via protein kinase C activation in cardiomyocytes. Anesthesiology 2003; 98:1363-71; PMID:12766644; http://dx.doi.org/10.1097/00000542-200306000-00010